^{57}Fe Mössbauer spectroscopy of $HoErFe_{17-x}Ga_xC_y$ compounds

M. Venkatesan,[1,2] U. V. Varadaraju,[1] and K. V. S. Rama Rao[2]
[1]*Materials Science Research Centre, Indian Institute of Technology, Madras 600 036, India*
[2]*Department of Physics, Indian Institute of Technology, Madras 600 036, India*
(Received 29 November 2000; published 14 August 2001)

^{57}Fe Mössbauer studies were carried out on the phases $HoErFe_{17-x}Ga_x$ ($x=0-7$) and $HoErFe_{17-x}Ga_xC$ ($x=0$, 1, and 2) at 25 K and room temperature. The weighted average hyperfine field at room temperature is found to increase initially for low Ga content and then decreases for phases with higher Ga concentration. The hyperfine fields at Fe sites follow the sequence $4f(6c)>6g(9d)>12j(18f)>12k(18h)$, which is determined mostly by the number of Fe and *R* nearest neighbors. The variation of the weighted average hyperfine field with temperature is found to obey T^2 behavior, suggesting the presence of single-particle excitations. Insertion of carbon at interstitial sites is found to increase the individual site hyperfine fields and hence an increase in the weighted average hyperfine field. The $12j$ and $12k$ sites of Fe show significant increase in isomer shift compared to other Fe sites.

DOI: 10.1103/PhysRevB.64.094427 PACS number(s): 76.80.+y, 71.20.Lp, 61.72.Ji

I. INTRODUCTION

Many studies have been devoted to study the structure of the $R_2Fe_{17-x}M_xA_y$ ($M=$Al, Ga, Si; $A=$C, N) in order to understand the relation between structure and magnetic properties since it is well established that the most effective way of increasing the Curie temperature and anisotropy of R_2Fe_{17} compounds is to synthesize interstitial or substitutional solid solutions.[1–7] The $4f$ sites of Fe play an important role in determining the magnetic properties of the R_2Fe_{17} compounds and their interstitial solid solutions.[8] Recently, we have reported on the structural and magnetic properties of $HoErFe_{17-x}Ga_x$ compounds[9] and their carbides[10] which contain rare earths with a mixture of positive (Er) and negative (Ho) Steven's factor. Detailed neutron diffraction studies were also performed on these compounds.[11] The incorporation of carbon in R_2Fe_{17} lattices leads to an increase in the Curie temperature through lattice expansion. A similar mechanism is thought to be responsible for the increase in the Curie temperature in nonmagnetic atom substituted R_2Fe_{17} compounds. In R_2Fe_{17} compounds, the magnetic anisotropy of the rare-earth sublattice shows a different temperature dependence from that of the Fe sublattice. Thus the compounds may exhibit a change in magnetic anisotropy as the temperature is varied. The decrease in rare-earth sublattice anisotropy with increasing temperature, in general, is steeper than that of an iron sublattice, resulting in a change of the sign of the total anisotropy at a temperature below T_C. To examine the change of the easy magnetization direction at low temperature and as part of a comprehensive study of the effect of combined substitutional-interstitial modification on the structure and magnetic properties of the rare-earth-based R_2Fe_{17} compounds, Mössbauer spectroscopy studies, which probe on a microscopic basis the iron atoms on the four inequivalent crystallographic sites, were carried out at both room temperature and low temperature. We report here the results obtained from ^{57}Fe Mössbauer studies carried on $HoErFe_{17-x}Ga_x$ ($x=0-7$) and their carbides $HoErFe_{17-x}Ga_xC$ ($x=0-2$). The variations in hyperfine parameters with Ga substitution at Fe sites and with carbon at the interstitial sites and the temperature dependence of hyperfine parameters are also discussed.

II. EXPERIMENT

The compounds $HoErFe_{17-x}Ga_x$ ($x=0-7$) were prepared by arc melting the constituent elements (Ho, Er, Ga: 99.9%; Fe: 99.99%) in high-purity Ar atmosphere. The ingots were wrapped in Ta foil, sealed in quartz ampoules under a pressure of 10^{-6} torr, annealed at 900 °C for 1 week, and subsequently slow cooled to room temperature. To synthesize carbides $HoErFe_{17-x}Ga_xC$ ($x=0-2$), due to the high melting point of carbon, Fe and C were melted together first to form Fe_3C (Cementite), which has a lower melting temperature. The alloy was then melted with the remaining constituent elements to form an ingot. The ingots were wrapped in Ta foils and subsequently annealed at 1100 °C for 3 days. In order to avoid the formation of a $R_2Fe_{14}C$ phase during cooling, the ingots were quenched into an ice-water mixture. The phases were characterized by powder x-ray diffraction using Cr$K\alpha$ ($\lambda=2.289$ Å) radiation. Mössbauer spectra were recorded using a conventional constant-acceleration spectrometer with a 20-mCi ^{57}Co source in a Rh matrix. The spectrometer was calibrated with α-Fe at room temperature. The Mössbauer absorbers were in the form of powder, with a dimension of about 30 mg/cm^2. The recording time depends on the concentration of Fe in the compound. In the present study, the minimum recording time was around 12 h and maximum around 48 h. The temperature-variation studies were carried out in the range 300–25 K with the help of a closed-cycle helium refrigerator, which is interfaced with the Mössbauer spectrometer.[12] The sample chamber was filled with helium gas at a pressure of 1 atm. The temperature of the sample was monitored using a carbon glass resistor as temperature sensor.

III. RESULTS AND DISCUSSION

^{57}Fe Mössbauer studies have been carried out on the phases $HoErFe_{17-x}Ga_xC_y$ at both room temperature and 25

K. The aim of this study is to investigate the variation of hyperfine fields at crystallographically inequivalent Fe sites upon Ga substitution and carbon insertion. The variation of isomer shifts and quadrupole splitting at various sites were also analyzed. The spin-reorientation transitions observed in carbonated compounds through ac magnetic susceptibility measurements[13] were used for assignment of sextets in analyzing the Mössbauer spectra at 25 K. The assignment of hyperfine parameters to the different sextets and the fitting procedures are also presented.

A. Analysis of the Mössbauer spectra

The obtained Mössbauer spectra are fitted and analyzed using the PCMOS least-squares refinement program. As there are four different crystallographic sites for Fe in both the hexagonal and rhombohedral-type R_2Fe_{17} compounds, the observed spectrum must be a superposition of at least four sextets. The different Fe sites in the hexagonal and rhombohedral (in brackets) structures are denoted as $4f(6c)$, $6g(9d)$, $12j(18f)$, and $12k(18h)$. Point-charge calculations[14] showed that under the combined effect of the dipolar field and quadrupole interaction, only the dumbbell $4f(6c)$ sites remain equivalent since the angle between the hyperfine field and the electric field gradient tensor is zero. The hyperfine parameters are different at various crystallographically inequivalent sites. When the magnetization direction is along the *c* axis, the angle between the hyperfine field and the electric field gradient is the same for all crystallographically inequivalent sites and hence there is no additional splitting and the sites remain equivalent for both structures. When the magnetization direction lies in the basal plane, for the rhombohedral structure, the $9d$, $18f$, and $18h$ sites each splits into two groups with an intensity ratio 2:1; while in the hexagonal structure, the $6g$ and $12k$ sites split into two groups with an intensity ratio 2:1 and the $12j$ site splits into three groups with an intensity ratio 1:1:1. Since the dipolar fields at two of the three groups of the $12j$ sites are very close, they can be treated in the same way as the $18f$ site in the rhombohedral compounds. In other words, because of the differences in the angle between the magnetization direction and the direction of the main axis of the electric field gradient tensor, the crystallographically equivalent iron atoms of a given subgroup will become magnetically nonequivalent. This leads to a total number of seven subspectra with intensity ratio 4(6):4(6):2(3):8(12):4(6):8(12):4:(6).[15,16]

In the present study, due to large number of sextets, some constraints were adopted during the process of fitting. As the sample was not subjected to any external magnetic field, the intensities of the six absorption lines of each of the sextets were assumed to obey the 3:2:1 intensity ratio. The relative intensity ratios for each of the special components were constrained to nearly 4(6):6(9):12(18):12(18), corresponding to the site occupancy of Fe atoms in the crystal structure. The isomer shifts for the magnetically inequivalent sites were constrained to be the same, whereas the hyperfine fields are expected to be slightly different at pairs of magnetically inequivalent sites as a result of variations in the dipolar and orbital contributions to the magnetic hyperfine fields. A single common linewidth was assumed for all the seven sextets.[17,18]

B. $HoErFe_{17-x}Ga_x$ ($x=0,1,2,3,4,5,6,7$)

^{57}Fe Mössbauer spectra have been recorded for these compounds at both room temperature and 25 K. Since the compounds possess planar anisotropy at room temperature, as confirmed by x-ray diffraction studies on magnetically oriented samples, the magnetic moments lie in the basal plane of the unit cell. Therefore, the four inequivalent crystallographic sites for Fe split into seven inequivalent magnetic sites and are designated as $4f(6c)$, $6g_1(9d_1)$, $6g_2(9d_2)$, $12j_1(18f_1)$, $12j_2(18f_2)$, $12k_1(18h_1)$, and $12k_2(18h_2)$. Figures 1(a), 1(b) and 2(a), 2(b) show the Mössbauer spectra obtained at room temperature and 25 K, respectively. Due to the presence of multiple sextets, the spectra are quite complex. Based on neutron diffraction and Mössbauer studies on the compounds in the present investigation and also by comparing the data available in the literature on isostructural compounds,[11,19] the percentage occupation of Ga atoms at crystallographically inequivalent Fe sites is summarized in Table I. It is evident that the compounds with $x=0-4$ crystallize in the hexagonal unit cell and Ga atoms occupy $12j$ and $12k$ sites. Compounds with $x\geqslant 5$ crystallize in rhombohedral structure. For $x=5$, Ga atoms occupy the equivalent $18f$ and $18h$ sites in rhombohedral structure. For compounds with $x>5$, Ga starts to occupy the dumbbell $6c$ site in the rhombohedral structure. It is interesting to note that, at high Ga concentration, the occupancy is more at $18f$ sites compared to $18h$ sites.

C. Effect of Ga substitution on hyperfine fields

Table II presents the hyperfine fields and the weighted average values at various magnetically inequivalent Fe sites of $HoErFe_{17-x}Ga_x$ compounds at 25 K and room temperature (brackets), respectively. It can be noted that with increasing Ga concentration, there is an initial increase in the weighted average hyperfine fields at room temperature, which reaches a maximum for phases with $x=1$ and then decreases with further increase in Ga content. The variation of the weighted average hyperfine fields is shown in Fig. 3. The behavior resembles the trend of room-temperature magnetization in Ga substituted compounds.[10] But the range of concentration of the Ga at which the hyperfine field and magnetization peaks is different. This behavior is well explained by invoking the concepts of chemical effect (charge transfer from the valence band of Ga to the $3d$ band of Fe) and the magnetic dilution effect. The reduction in hyperfine fields at higher Ga content is mainly due to magnetic dilution. Hyperfine fields at various Fe sites are in the order

$$H_{\mathrm{hf}}[4f(6c)]>H_{\mathrm{hf}}[6g(9d)]>H_{\mathrm{hf}}[18f(12j)]>H_{\mathrm{hf}}[12k(18h)],$$

which agrees well with other studies.[16] The hyperfine splitting of the dumbbell site $4f(6c)$ is larger than those of the other three sites. The strength of the hyperfine field at each

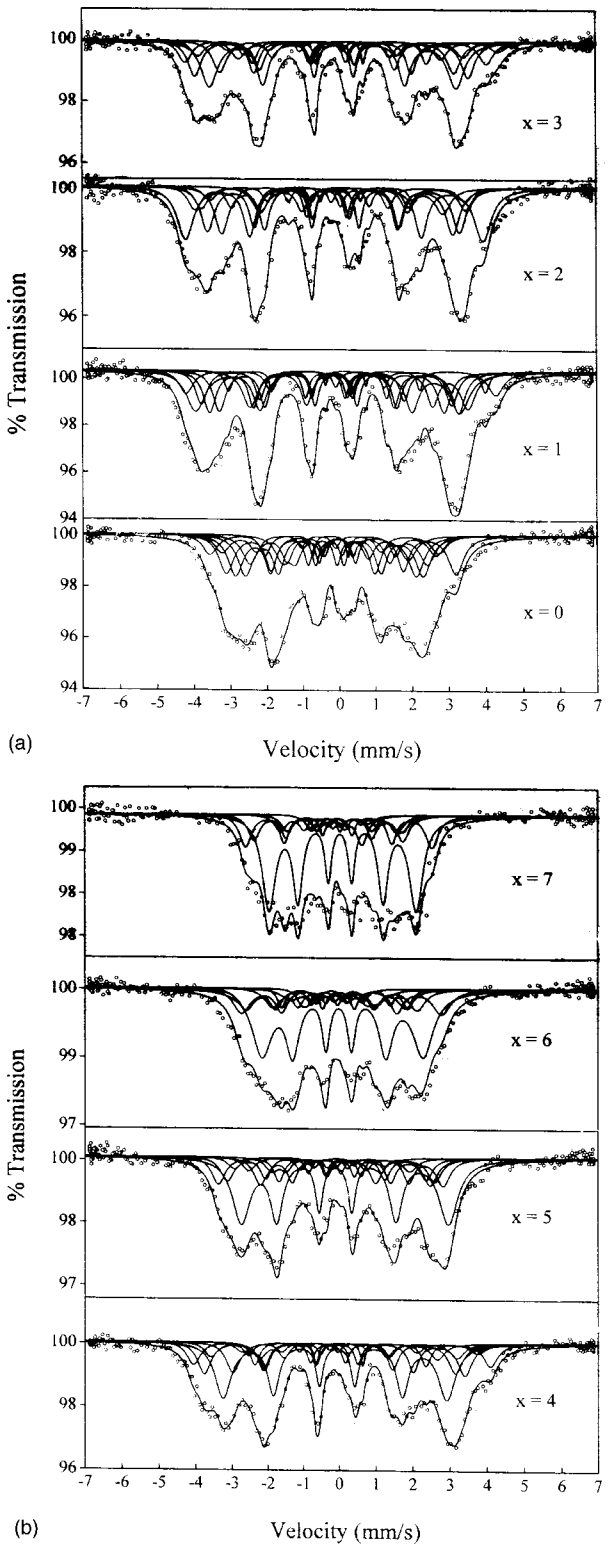

FIG. 1. (a) Mössbauer spectra of $HoErFe_{17-x}Ga_x$ $(x=0-3)$ at 300 K. (b) Mössbauer spectra of $HoErFe_{17-x}Ga_x$ $(x=4-7)$ at 300 K.

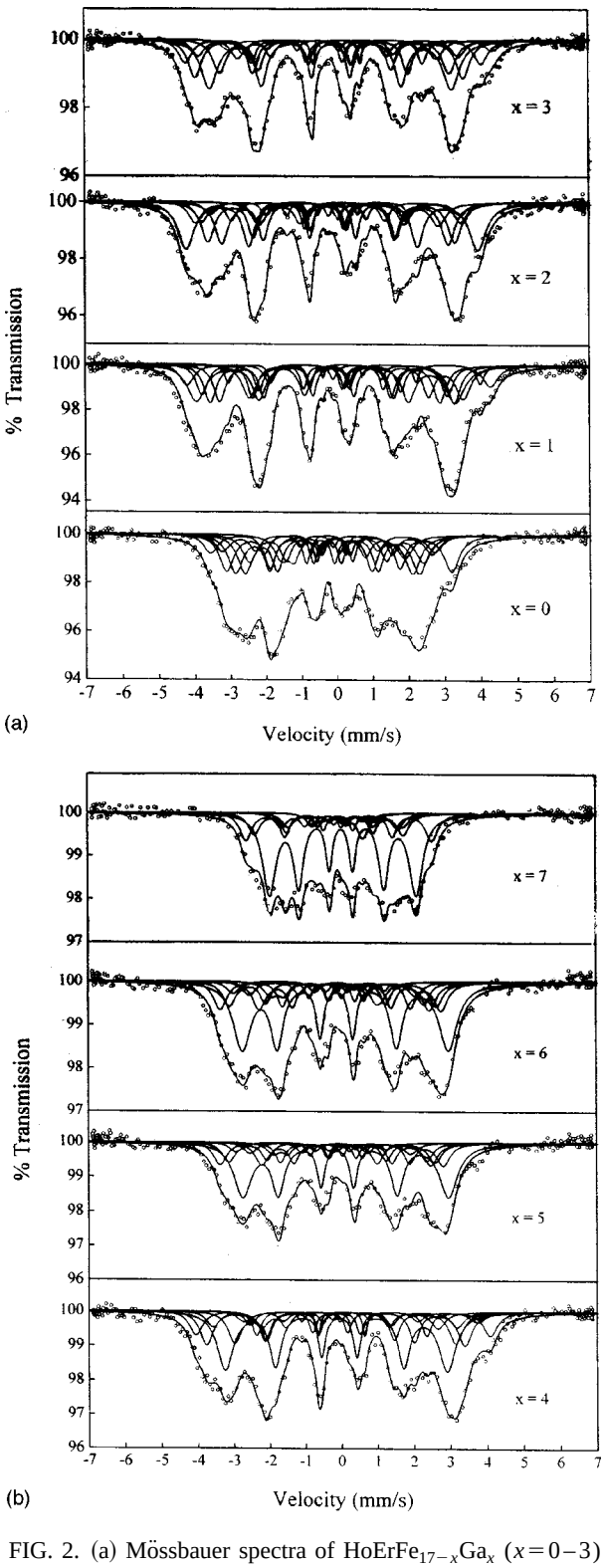

FIG. 2. (a) Mössbauer spectra of $HoErFe_{17-x}Ga_x$ $(x=0-3)$ at 25 K. (b) Mössbauer spectra of $HoErFe_{17-x}Ga_x$ $(x=4-7)$ at 25 K.

site is predominantly determined by the number of iron and rare-earth nearest neighbors of the site. The higher the number of iron neighbors, the larger is the hyperfine field, whereas the higher the number of rare-earth neighbors, the smaller is the hyperfine field. The magnitude of the hyperfine field is directly correlated to the number of nearest-neighbor Fe atoms. The number of nearest-neighbor Fe atoms at different sites are listed in Table III. The number of Fe neighbors for $4f(6c)$, $6g(9d)$, $12j(18f)$, and $12k(18h)$ are 13, 10, 10, and 9, respectively.[20] So, in $HoErFe_{17-x}Ga_x$ com-

TABLE I. Occupancy of Ga atoms (%) at crystallographically inequivalent Fe sites in $HoErFe_{17-x}Ga_x$ ($x=0-7$) compounds.

x	$4f$ ($6c$)	$6g$ ($9d$)	$12j$ ($18f$)	$12k$ ($18h$)
0	0	0	0	0
1	0	0	4.8	11.5
2	0	0	14.2	18.7
3	0	0	18.3	31.3
4	0	0	31.8	35.2
5	0	0	43.2	39.6
6	25.2	0	57.2	35.6
7	77.3	0	63.8	28.1

pounds, there are $(13-x)$ Fe nearest neighbors for Fe $4f(6c)$ sites, $(10-x)$ for Fe $6g(9d)$ and $12j(18f)$ sites, and $(9-x)$ for Fe $12k(18h)$ sites depending on the occupation of Ga at Fe sites. Since the $4f(6c)$ site has a large number of Fe nearest neighbors, it is reasonable to expect the highest hyperfine field for this site. Similarly, the $12k(18h)$ site has the lowest value for the hyperfine field as a consequence of the smallest number of Fe nearest neighbors. The Fe sites $6g(9d)$ and $12j(18f)$ have the same number of Fe nearest neighbors. But the Fe-Fe interatomic distances at the $6g(9d)$ site is somewhat smaller than that observed at $12j(18f)$ sites and hence a larger hyperfine field is observed at $6g(9d)$ sites than $12j(18f)$ sites. This attribution of hyperfine fields is consistent with neutron diffraction results on the Nd_2Fe_{17} compound[21] and band structure calculations on Y_2Fe_{17}.[22] It is clear from Table II that there is a difference in hyperfine fields between magnetically inequivalent sites

TABLE II. Magnetic hyperfine fields (±1 kOe) and the weighted average values (±1 kOe) for $HoErFe_{17-x}Ga_x$ at 25 K and 300 K (in parentheses).

x	$4f$ ($6c$) (kOe)	$6g_1$ ($9d_1$) (kOe)	$6g_2$ ($9d_2$) (kOe)	$12j_1$ ($18f_1$) (kOe)	$12j_2$ ($18f_2$) (kOe)	$12k_1$ ($18h_1$) (kOe)	$12k_2$ ($18h_2$) (kOe)	Average (kOe)
0	237	221	209	192	173	172	156	191
	(184)	(171)	(167)	(161)	(155)	(152)	(146)	(160)
1	235	225	211	190	175	176	163	192
	(207)	(178)	(171)	(165)	(159)	(154)	(151)	(167)
2	229	217	208	187	176	168	160	189
	(198)	(166)	(160)	(152)	(147)	(137)	(132)	(152)
3	217	206	203	182	174	162	153	182
	(196)	(163)	(158)	(149)	(143)	(133)	(130)	(151)
4	203	192	184	169	163	148	141	169
	(188)	(159)	(151)	(147)	(140)	(130)	(121)	(146)
5	192	174	168	154	151	136	124	155
	(177)	(155)	(147)	(145)	(139)	(128)	(113)	(143)
6	161	157	143	139	132	129	118	138
	(148)	(136)	(123)	(125)	(113)	(113)	(104)	(122)
7	138	134	123	130	126	114	103	121
	(126)	(116)	(108)	(104)	(97)	(93)	(81)	(100)

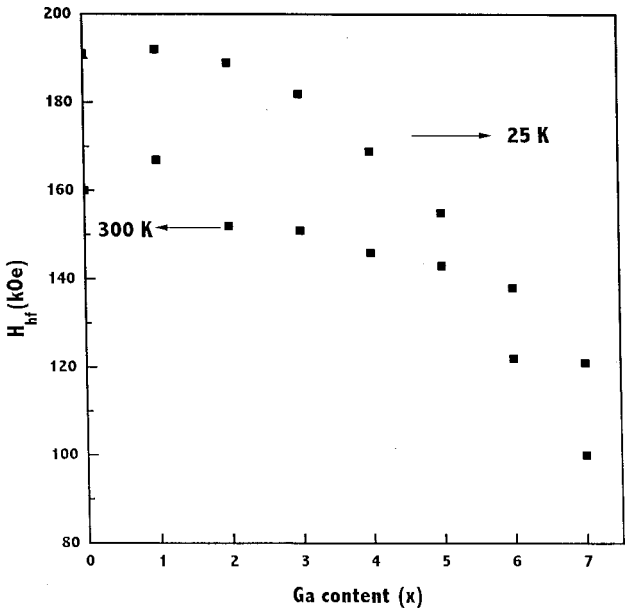

FIG. 3. Variation of the weighted average hyperfine field with Ga content in $HoErFe_{17-x}Ga_x$ ($x=0-7$) at 25 and 300 K.

$[4f(6c),\ 6g_1(9d_1),\ 6g_2(9d_2),\ 12j_1(18f_1),\ 12j_2(18f_2),\ 12k_1(18h_1)$, and $12k_2(18h_2)]$.

In order to determine the variation of hyperfine field with temperature, the Mössbauer spectra were recorded for the compound $HoErFe_{15}Ga_2$ at different temperatures (25, 100, 200, and 300 K). The temperature dependence of the average hyperfine field (weighted average of the contribution from different Fe sites) was analyzed in terms of different power laws of the reduced temperature. The reduced hyperfine fields can be expressed as

$$\frac{H_{\mathrm{eff}}(T)}{H_{\mathrm{eff}}(0)}=\left\{1-b\left(\frac{T}{T_c}\right)^2\right\}. \tag{1}$$

The variation of the hyperfine field with temperature fits very well to Eq. (1) as shown in Fig. 4. The value of the hyperfine field at 25 K has been taken as $H_{\mathrm{hf}}(0)$. The value of the constant b is 0.53. It has been reported that in Y_2Fe_{17},

TABLE III. Number of Fe and R neighbors for Fe atoms at various crystallographic sites in R_2Fe_{17} compounds.

Site	$4f(6c)$	$6g(9d)$	$12(18f)$	$12k(18h)$	$2b,2d(6c)$
$4f(6c)$	1	3	6	3	1
$6g(9d)$	2	0	4	4	2
$12(18f)$	2	2	2	4	2
$12k(18h)$	1	2	4	2	3

Site	Number of Fe neighbors	Number of rare-earth neighbors
$4f(6c)$	13	1
$6g(9d)$	10	2
$12j(18f)$	10	2
$12k(18h)$	9	3

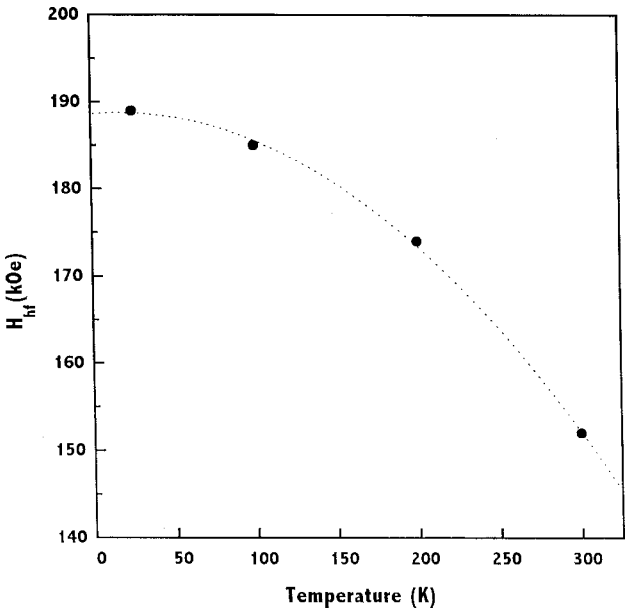

FIG. 4. Temperature variation of the weighted average hyperfine field in $HoErFe_{15}Ga_2$.

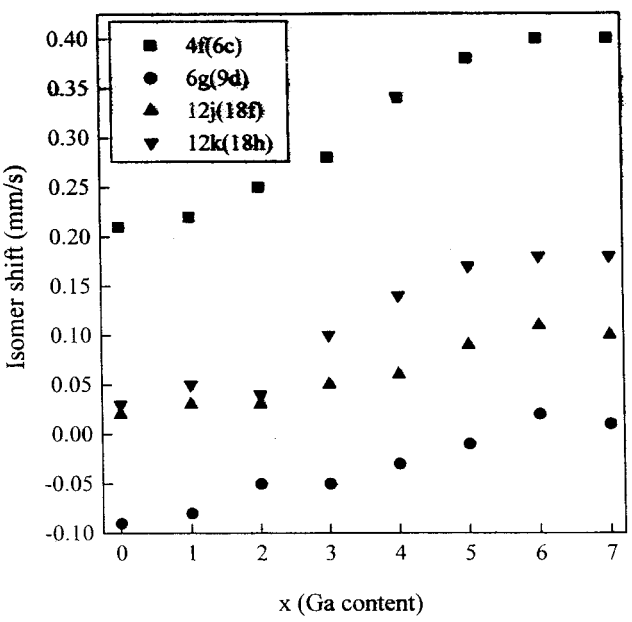

FIG. 5. Variation of the isomer shift at crystallographically inequivalent Fe sites in $HoErFe_{17-x}Ga_x$ ($x=0-7$) at 25 K.

Nd_2Fe_{17}, and Dy_2Fe_{17}, the temperature dependence of the hyperfine fields follows the above equation with a constant $b=0.5$.[23,24] The temperature dependence of the magnetization of ferromagnetic metals is also found to obey T^2 behavior. This kind of T^2 behavior is usually attributed to the presence of single-particle excitations. Based on these arguments, one can conclude that, due to direct relationship between the hyperfine field and Fe magnetic moment, single-particle excitations are responsible for the reduction in magnetization with temperature in these compounds.

Isomer shifts at different inequivalent Fe sites indicating the variations in the chemical environment at the Fe nucleus are presented in Table IV. The isomer shift increases with the increasing Ga concentration. The charge transfer between the valence band of Ga and the $3d$ band of Fe may probably result in a $3d$-$4s$ intraatomic charge redistribution. This, in turn, reduces the s-electron density at the Fe nucleus. This will lead to an increase in the isomer shift. Similar behavior is reported in Al-substituted R_2Fe_{17} compounds.[25]

The variation of isomer shifts at different sites with Ga

TABLE IV. Isomer shifts ($\pm$0.01 mm/s) at various Fe sites in $HoErFe_{17-x}Ga_x$ at 25 K and 300 K (in parentheses).

x	$4f$ ($6c$) (mm/s)	$6g_1$ ($9d_1$) (mm/s)	$6g_2$ ($9d_2$) (mm/s)	$12j_1$ ($18f_1$) (mm/s)	$12j_2$ ($18f_2$) (mm/s)	$12k_1$ ($18h_1$) (mm/s)	$12k_2$ ($18h_2$) (mm/s)
0	0.21	−0.09	−0.09	0.02	0.02	0.03	0.03
	(0.10)	(−0.15)	(−0.15)	(−0.04)	(−0.04)	(−0.05)	(−0.05)
1	0.22	−0.08	−0.08	0.03	0.03	0.05	0.05
	(0.10)	(−0.07)	(−0.07)	(−0.01)	(−0.01)	(−0.02)	(−0.02)
2	0.25	−0.05	−0.05	0.03	0.03	0.04	0.04
	(0.11)	(−0.06)	(−0.06)	(−0.01)	(−0.01)	(0.01)	(0.01)
3	0.28	−0.05	−0.05	0.05	0.05	0.10	0.10
	(0.14)	(−0.03)	(−0.03)	(0.01)	(0.01)	(0.05)	(0.05)
4	0.34	−0.03	−0.03	0.06	0.06	0.14	0.14
	(0.16)	(−0.01)	(−0.01)	(0.04)	(0.04)	(0.10)	(0.10)
5	0.38	−0.01	−0.01	0.09	0.09	0.17	0.17
	(0.21)	(0.02)	(0.02)	(0.13)	(0.13)	(0.11)	(0.11)
6	0.40	0.02	0.02	0.11	0.11	0.18	0.18
	(0.24)	(0.04)	(0.04)	(0.12)	(0.12)	(0.15)	(0.15)
7	0.40	0.01	0.01	0.10	0.10	0.18	0.18
	(0.27)	(0.05)	(0.05)	(0.12)	(0.12)	(0.16)	(0.16)

TABLE V. Quadrupole splittings ($\pm$0.01 mm/s) at different Fe sites for $HoErFe_{17-x}Ga_x$ at 25 K and 300 K (in parentheses).

x	$4f$ ($6c$) (mm/s)	$6g_1$ ($9d_1$) (mm/s)	$6g_2$ ($9d_2$) (mm/s)	$12j_1$ ($18f_1$) (mm/s)	$12j_2$ ($18f_2$) (mm/s)	$12k_1$ ($18h_1$) (mm/s)	$12k_2$ ($18f_2$) (mm/s)
0	−0.04	−0.06	0.32	0.28	−0.13	−0.21	0.38
	(−0.02)	(0.10)	(0.30)	(0.17)	(−0.09)	(−0.34)	(0.32)
1	−0.09	−0.08	0.34	0.07	−0.12	−0.09	0.37
	(−0.03)	(−0.14)	(0.30)	(0.03)	(−0.09)	(−0.23)	(0.33)
2	−0.14	−0.16	0.33	−0.05	−0.12	0.06	0.37
	(−0.04)	(−0.18)	(0.31)	(0.01)	(−0.09)	(−0.18)	(0.34)
3	−0.17	−0.17	0.36	0.09	−0.11	0.08	0.36
	(−0.06)	(−0.22)	(0.28)	(0.03)	(−0.06)	(−0.22)	(0.34)
4	−0.20	−0.17	0.36	0.16	−0.13	0.09	0.37
	(−0.09)	(−0.19)	(0.29)	(0.06)	(−0.10)	(0.22)	(0.33)
5	−0.23	−0.14	0.35	0.14	−0.09	0.07	0.45
	(−0.12)	(−0.19)	(0.29)	(0.05)	(−0.05)	(0.19)	(0.43)
6	−0.27	−0.13	0.35	0.23	−0.10	0.05	0.45
	(−0.14)	(−0.14)	(0.27)	(0.05)	(−0.05)	(0.17)	(0.44)
7	−0.30	−0.08	0.34	−0.02	−0.09	0.05	0.46
	(−0.14)	(−0.10)	(0.26)	(−0.15)	(−0.04)	(0.15)	(0.43)

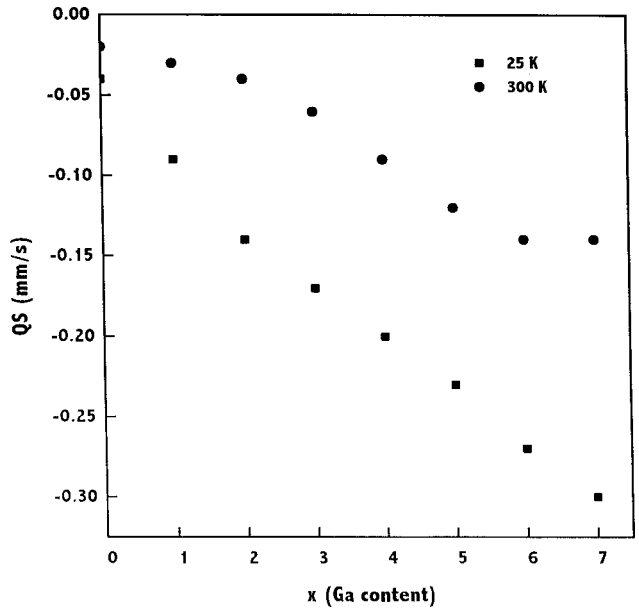

FIG. 6. Variation of the quadrupole splitting at the Fe ($4f$) site in $HoErFe_{17-x}Ga_x$ ($x=0-7$) at 25 and 300 K.

content is shown in Fig. 5. It is noteworthy that the iron $4f(6c)$ site has a larger isomer shift and the $6g(9d)$ site has a lower isomer shift. In R_2Fe_{17} phases, the Wigner-Seitz cell volume is the largest for Fe $4f(6c)$ site, whereas it is the smallest for the $6g(9d)$ site.[26] Therefore, the *s*-electron density at the nucleus will be smallest at the Fe $4f(6c)$ site and largest at the $6g(9d)$ site. Since the isomer shift is directly proportional to the negative of the *s*-electron density at the Fe nucleus, it has larger value at the $4f(6c)$ site compared to the $6g(9d)$ site.

The quadrupole splittings for $HoErFe_{17-x}Ga_x$ compounds at different magnetically inequivalent Fe sites at 25 K and room temperature (brackets) are presented in Table V. In R_2Fe_{17} compounds, the angle between the principal component of the electric field gradient tensor and the hyperfine field is known only for the $4f(6c)$ site. The direction of the principal component of the electric field gradient is not known for other three sites, viz., $6g$, $12j$, and $12k$ sites. Therefore, the observed quadrupole splitting for $4f(6c)$ corresponds to e^2Qq and is plotted in Fig. 6. The substitution of Ga changes the magnitude and sign of the quadrupole splitting at various Fe sites. In particular, there are large variations in the values for the $12j_1(18f_1)$ and $12k_1(18h_1)$ sites.

D. $HoErFe_{17-x}Ga_xC$ ($x=0$, 1, and 2)

^{57}Fe Mössbauer spectra were recorded at 25 K and room temperature for the carbides $HoErFe_{17-x}Ga_xC$ ($x=0$, 1, and 2). It is established through ac magnetic susceptibility measurements[13] that the easy magnetization direction lies in the basal plane of the unit cell at room temperature, whereas it is oriented along the *c* axis at 25 K. Figures 7(a) and 7(b) show the Mössbauer spectra of $HoErFe_{17-x}Ga_xC$ ($x=0$, 1, and 2) compounds at room temperature and 25 K, respectively. The spectra of all compounds were fitted into seven independent sextets at room temperature due to the planar

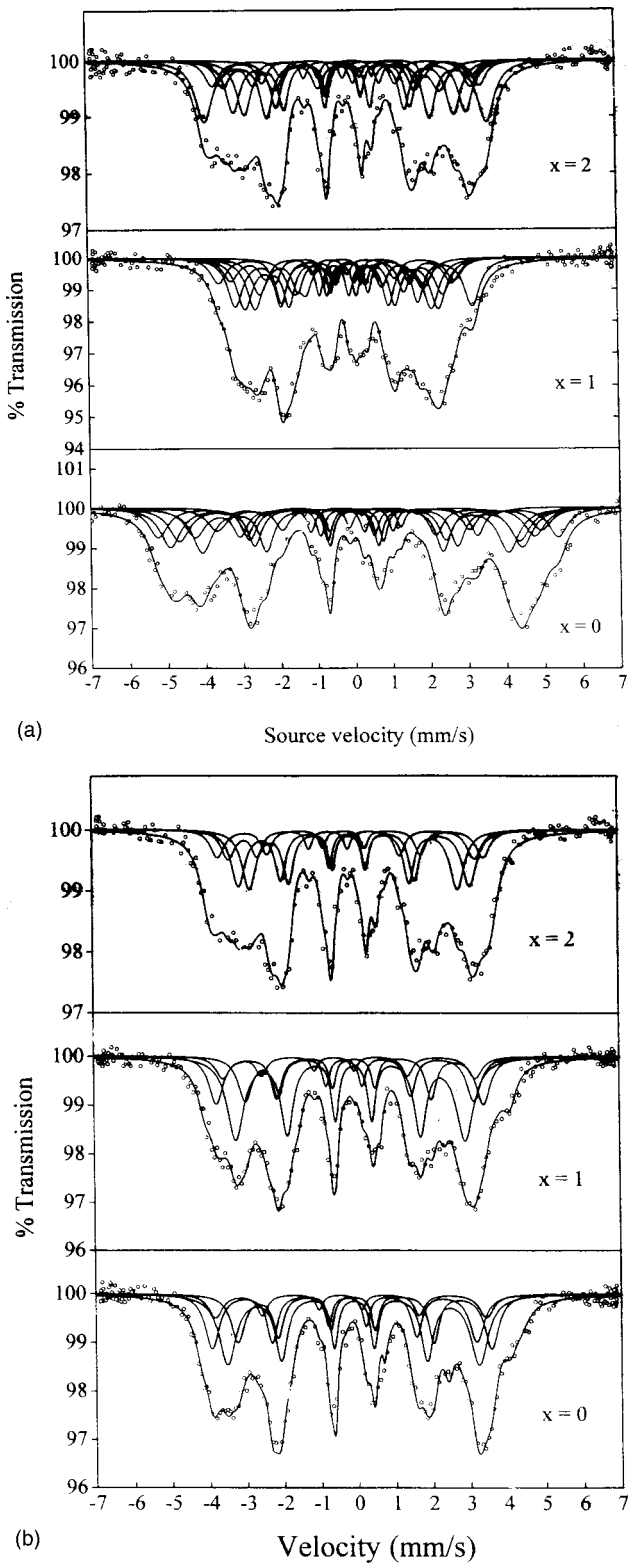

FIG. 7. (a) Mössbauer spectra of $HoErFe_{17-x}Ga_xC$ ($x=0,1,2$) compounds at 300 K. (b) Mössbauer spectra of $HoErFe_{17-x}Ga_xC$ ($x=0,1,2$) compounds at 25 K.

anisotropy exhibited by these compounds. Since the compounds show a spin-reorientation transition (43 K for $HoErFe_{17}C$, 50 K for $HoErFe_{16}GaC$, and 31 K for

TABLE VI. (a) Weighted average hyperfine field (±1 kOe) and (b) isomer shift (±0.01 mm/s) at Fe sites in $HoErFe_{17-x}Ga_xC$ at 25 K and 300 K (in parentheses).

(a) x	$4f$ (kOe)	$6g$ (kOe)	$12j$ (kOe)	$12k$ (kOe)	Average (kOe)
0	263	248	213	183	214
	(224)	(201)	(186)	(164)	(185)
1	255	234	201	179	201
	(226)	(190)	(183)	(164)	(178)
2	252	233	201	180	196
	(218)	(183)	(177)	(165)	(169)

(b) x	$4f$ (mm/s)	$6g$ (mm/s)	$12j$ (mm/s)	$12k$ (mm/s)
0	0.22	−0.12	0.09	0.15
	(0.07)	(−0.14)	(0.02)	(0.05)
1	0.23	−0.05	0.08	0.11
	(0.09)	(−0.08)	(0.01)	(0.02)
2	0.26	−0.04	0.16	0.08
	(0.12)	(−0.08)	(0.01)	(0.01)

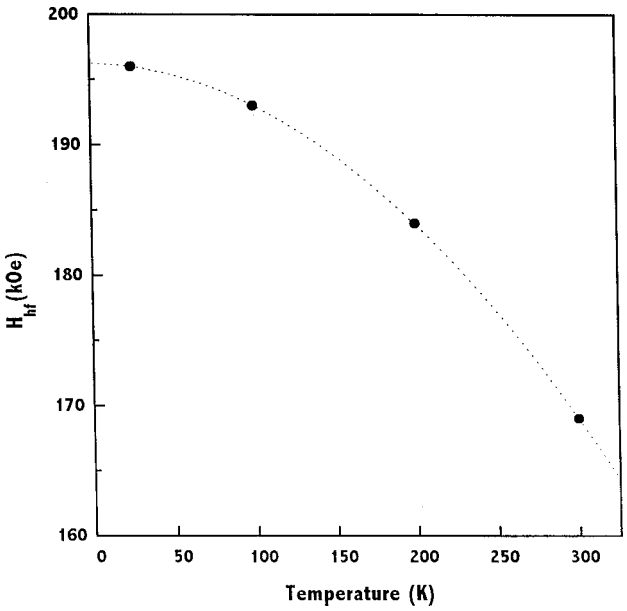

FIG. 8. Temperature variation of the weighted average hyperfine field in $HoErFe_{15}Ga_2C$.

$HoErFe_{15}Ga_2C$), as confirmed by ac magnetic susceptibility,[13] the spectra were fitted into four sextets ($4f$, $6g$, $12j$, and $12k$). The population of Fe at each site is assumed to be the same as in the Ga-substituted compounds.

Table VI(a) presents the hyperfine fields at various Fe sites together with the weighted average values. The hyperfine fields at various Fe sites and hence the average hyperfine field increase slightly with carbon insertion. The incorporation of carbon into the lattice gives rise to an increase in volume and associated with this is a sharp increase in T_C. According to the spin-polarized electron band structure calculation,[27] a relative change in volume gives rise to a relative increase in the average magnetic moment. It has been found that the average hyperfine fields are nearly proportional to the average iron moment.[28] As a consequence of this, the hyperfine field increases with carbon insertion. On the other hand, the hyperfine field decreases with increasing Ga content as a result of the reduction in the number of Fe atoms. Similar to $HoErFe_{15}Ga_2$, Mössbauer spectra were recorded for the compound $HoErFe_{15}Ga_2C$ at various temperatures to determine the variation of the hyperfine field. The temperature variation of the weighted average hyperfine field is plotted in Fig. 8 and is found to follow the Eq. (1) ($b=0.51$) similar to that observed in Ga-substituted phases.

The isomer shifts of $HoErFe_{17-x}Ga_xC$ ($x=0$, 1, and 2) at various Fe sites are presented in Table VI(b). All four isomer shifts increase upon carbonation. The influence of carbonation on the $12j$ and $12k$ sites, which have one nearest-neighbor carbon atom each, is more pronounced than on the $6c$ and $9d$ sites, which have no nearest-neighbor carbon atom. The assignment of the isomer shift is based on the Wigner-Seitz cell volumes[29] for the crystallographically inequivalent $4f$, $6g$, $12j$, and $12k$ sites. The Fe $4f(6c)$ site has the largest isomer shift, in agreement with its smallest Wigner-Seitz volume. The sequences of isomer shifts and Wigner-Seitz cell volumes, $4f>12k>12j>6g$, are identical.

The effect of carbonation on the isomer shift can be explained on either the basis of the weighted average isomer shift or isomer shifts of the individual sites. The expansion of the unit-cell volume due to carbonation increases the Wigner-Seitz cell volume of each site. This overall expansion of the lattice results in the well-known volume effect on the weighted average isomer shift, thereby decreasing the electron density at the iron nucleus. This accounts for the increase in the observed isomer shift. On the other hand, both the number of interstitial carbon atoms and the effect of carbon on the volume expansion need to be considered in explaining the isomer shift of an individual iron site. However, the $4f$ and $6g$ sites have no nearest-neighbor carbon atoms and hence the isomer shift depends solely on the increase in volume. The isomer shift at the $12j(18f)$ site where the iron is closest to the interstitial carbon shows an increase with carbon insertion.

IV. CONCLUSIONS

^{57}Fe Mössbauer studies were carried out on the phases $HoErFe_{17-x}Ga_x$ ($x=0-7$) and $HoErFe_{17-x}Ga_xC$ ($x=0$, 1, and 2) at 25 K and room temperature. The spectra obtained in Ga-substituted compounds were fitted to seven sextets as a result of the splitting of the $6g(9d)$, $12j(18f)$, and $12k(18h)$ sites into magnetically inequivalent sites. Since the carbides possess uniaxial anisotropy at 25 K and planar anisotropy at room temperature, the spectra were fitted well into four sextets at 25 K and seven sextets at room temperature. The weighted average hyperfine field at room temperature is found to increase initially for low Ga content and then decreases for phases with higher Ga concentration. The hy-

perfine fields at Fe sites follow the sequence $4f(6c) > 6g(9d) > 12j(18f) > 12k(18h)$, which is determined mostly by the number of Fe and *R* nearest neighbors. The variation of weighted average hyperfine field with temperature is found to obey T^2 behavior, suggesting the presence of single-particle excitations. The Fe $4f(6c)$ site has a larger isomer shift and the $6g(9d)$ site has a smaller isomer shift, suggesting that the *s*-electron density at the nucleus is smaller at the Fe $4f(6c)$ site and is larger at the $6g(9d)$ site. Insertion of carbon at interstitial sites is found to increase the individual site hyperfine fields and hence an increase in the weighted average hyperfine field. The $12j$ and $12k$ sites of Fe show a significant increase in the isomer shift compared to other Fe sites.

[1] J. M. D. Coey and H. Sun, J. Magn. Magn. Mater. **87**, L251 (1990).

[2] W. B. Yelon, H. Xie, G. J. Long, O. A. Pringle, F. Grandjean, and K. H. J. Buschow, J. Appl. Phys. **73**, 6029 (1993).

[3] M. Katter, J. Wecker, L. Schultz, and R. Grössinger, J. Magn. Magn. Mater. **92**, L14 (1990).

[4] H. Sun, B. P. Liu, H. S. Li, and J. M. D. Coey, Solid State Commun. **74**, 727 (1990).

[5] K. G. Suresh and K. V. S. Rama Rao, J. Appl. Phys. **79**, 345 (1996).

[6] B. P. Hu, X. L. Cao, J. M. Xu, G. C. Liu, F. Cao, X. L. Dong, H. Li, L. Yin, and Z. R. Zhao, J. Magn. Magn. Mater. **114**, 138 (1992).

[7] Z. H. Cheng, B. G. Shen, B. Liang, J. X. Zhang, F. W. Wang, S. Y. Zhang, J. G. Zhao, and W. S. Zhan, J. Appl. Phys. **78**, 1385 (1995).

[8] D. Givord and L. Lemaire, IEEE Trans. Magn. **MAG-10**, 109 (1974).

[9] M. Venkatesan, U. V. Varadaraju, and K. V. S. Rama Rao, in *Proceedings of the Third Pacific Rim International Conference on Advanced Materials and Processing (PRICM 3), Honolulu, Hawaii, 1998*, edited by M. A. Imam, R. DeNale, S. Hanada, Z. Zhong, and D. N. Lee (TMS, Warrendale, PA, 1998), p. 971.

[10] M. Venkatesan, U. V. Varadaraju, and K. V. S. Rama Rao, J. Magn. Magn. Mater. **184**, 231 (1998).

[11] M. Venkatesan, U. V. Varadaraju, K. V. S. Rama Rao, S. K. Malik, H. Luo, and W. B. Yelon, J. Appl. Phys. **86**, 3290 (1999).

[12] M. Senthil Kumar, K. V. Reddy, and K. V. S. Rama Rao, Meas. Sci. Technol. **7**, 965 (1996).

[13] M. Venkatesan, K. V. S. Rama Rao, and U. V. Varadaraju, Solid State Commun. **113**, 345 (1999).

[14] W. Steiner and R. Haferl, Phys. Status Solidi A **42**, 739 (1977).

[15] B. P. Hu, H. S. Li, H. Sun, and J. M. D. Coey, J. Phys.: Condens. Matter **3**, 3983 (1991).

[16] G. J. Long, O. A. Pringle, F. Grandjean, and K. H. J. Buschow, J. Appl. Phys. **72**, 4845 (1992).

[17] G. J. Long, G. K. Marasinghe, S. Mishra, O. A. Pringle, F. Grandjean, K. H. J. Buschow, D. P. Middleton, W. B. Yelon, F. Pourarian, and O. Isnard, Solid State Commun. **88**, 761 (1993).

[18] L. S. Kong, H. Y. Gong, B. G. Shen, L. Cao, and Y. L. Shen, Solid State Commun. **85**, 1011 (1993).

[19] G. K. Marasinghe, S. Mishra, O. A. Pringle, G. J. Long, Z. Hu, W. B. Yelon, F. Grandjean, D. P. Middleton, and K. H. J. Buschow, J. Appl. Phys. **76**, 6731 (1994).

[20] Q. N. Qi, H. Sun, R. Skomski, and J. M. D. Coey, Phys. Rev. B **45**, 12 278 (1992).

[21] J. F. Herbst, J. J. Croat, R. W. Lee, and W. B. Yelon, J. Appl. Phys. **53**, 250 (1982).

[22] B. Szpunar and J. A. Szpynar, J. Appl. Phys. **57**, 4130 (1985).

[23] P. C. M. Gubbens and K. H. J. Buschow, J. Phys. F: Met. Phys. **12**, 2715 (1982).

[24] J. J. M. Franse and R. J. Radwanski, in *Handbook of Magnetic Materials*, edited by K. H. J. Buschow (Elsevier, Amsterdam, 1993), Vol. 7, Chap. 7, pp. 307–501.

[25] G. J. Long, G. K. Marasinghe, O. A. Pringle, F. Grandjean, Z. Hu, W. B. Yelon, D. P. Middleton, K. H. J. Buschow, and F. Grandjean, J. Appl. Phys. **76**, 5383 (1994).

[26] G. J. Long, O. A. Pringle, F. Grandjean, and K. H. J. Buschow, J. Appl. Phys. **74**, 504 (1993).

[27] R. Coehoorn, Phys. Rev. B **39**, 13 072 (1989).

[28] G. J. Long and F. Grandjean, in *Supermagnets, Hard Magnetic Materials*, edited by G. J. Long and F. Grandjean (Kluwer Academic, Dordrecht, 1991), pp. 355–389.

[29] L. Gelato, J. Appl. Crystallogr. **14**, 141 (1981).